

# Cross-Linked Network Polymer Electrolytes Based on a Polysiloxane Backbone with Oligo(ethylene glycol) Side Chains: Synthesis and Conductivity

Zhengcheng Zhang, David Sherlock, Ryan West, and Robert West

Organosilicon Research Center, Department of Chemistry, University of Wisconsin–Madison, 1101 University Avenue, Madison, Wisconsin 53706

Khalil Amine

Chemical Technology Division, Argonne National Laboratory, Argonne, Illinois 60439

Leslie J. Lyons\*

Department of Chemistry, Grinnell College, Grinnell, Iowa 50112

Received July 2, 2003; Revised Manuscript Received September 25, 2003

**ABSTRACT:** A novel cross-linked siloxane-based solid polymer network has been synthesized by the hydrosilylation of polymethylhydrosiloxane (PMHS) partly substituted with oligo(ethylene glycol) methyl ether side groups and a  $\alpha,\omega$ -diallyl poly(ethylene glycol) cross-linking reagent. The ionic conductivities of the networks doped with LiTFSI are high at ambient temperature ( $\sigma = 1.33 \times 10^{-4} \text{ S cm}^{-1}$  at the optimum LiTFSI concentration EO/Li<sup>+</sup> = 20:1). The temperature dependence of the conductivity followed the VTF form, indicating that polymer segmental motion assists the ion transport in the solid networks.

## Introduction

Solid polymer electrolytes (SPEs) have been widely investigated since the discovery of ionic conductivity in the polyether/alkali metal complex PEO/KSCN by Wright et al. in the 1970s.<sup>1–3</sup> Recognizing that the ionic conductivity of polymer electrolytes is enhanced in the elastomeric amorphous phase by the segmental motion of the polymer chains, significant research has been undertaken to develop a polymer structure having a highly flexible backbone and amorphous character. Polymer electrolytes based on poly[bis(methoxyethoxyethoxy)phosphazene] (MEEP) which was studied as a polymer electrolyte by Shriver, Allcock, and their co-workers was a breakthrough in this area.<sup>4–8</sup> Complexes of MEEP doped with LiSO<sub>3</sub>CF<sub>3</sub> exhibit room temperature ionic conductivities of up to 3 orders of magnitude higher than those of analogous PEO complexes. The remarkable improvement in the ionic conductivity was ascribed to the highly flexible inorganic phosphazene backbone which produced a totally amorphous polymer host with a very low glass transition temperature.

The polysiloxanes, with very low glass transition temperatures,  $T_g = -123^\circ\text{C}$  for poly(dimethylsiloxane), and extremely high free volumes, are expected to be good hosts for Li<sup>+</sup> transport when polar units are introduced onto the polymer backbone. Oligo(ethylene glycol)-substituted polysiloxanes as ionically conductive polymer hosts have been previously investigated by Smid,<sup>9–11</sup> Shriver,<sup>12–14</sup> Acosta,<sup>15</sup> and West and co-workers.<sup>16,17</sup> The more recent synthesis and conductivity studies of a bis-substituted polysiloxane with pendant oligo(ethylene glycol) chains have been reported by Hooper et al.<sup>18</sup> A six-oxygen side-chain polymer host when doped with lithium bis(trifluoromethylsulfonyl)imide (LiTFSI) showed the highest room temperature conductivity ( $4.0 \times 10^{-4} \text{ S cm}^{-1}$ ) yet observed for a polymer electrolyte. However, the dimensional stability of these polymer electrolytes is poor. It is not possible

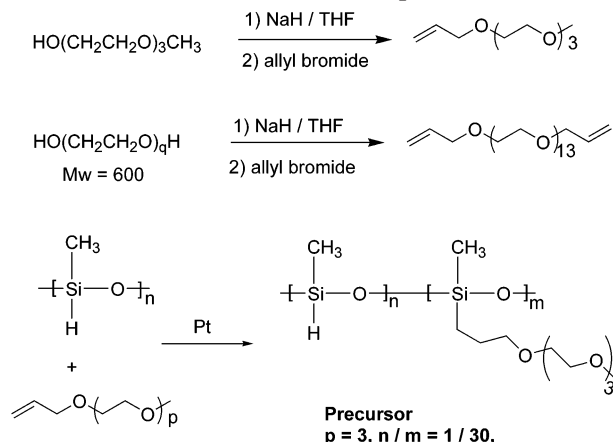
to use the complexes as separators in all solid-state lithium polymer batteries since the glutinous materials flow even under mild pressure at ambient temperature.

We now report the synthesis of a cross-linked polysiloxane network polymer electrolyte with pendant oligo(ethylene glycol) groups as internally plasticizing chains. This free-standing polysiloxane conductive material, when doped with LiTFSI, shows very high room temperature conductivity, contributed from the vigorous segmental motion of the pendant short PEO chains as well as the high flexibility of the siloxane backbone.

## Experimental Section

**Materials.** Polymethylhydrosiloxane (PMHS,  $M_w = 1500$ –1900) was purchased from Gelest. Tri(ethylene glycol) methyl ether (MPEO<sub>3</sub>) and poly(ethylene glycol) ( $M_w$  600) were Aldrich products. All were dried by using 4A molecular sieves. Allyl bromide and platinum divinyltetramethyldisiloxane [Pt(dvs)], 3% in xylene solution were supplied by Aldrich also. Sodium hydride (NaH, 60% dispersion in mineral oil) was purchased from Acros Organics. THF was dried over sodium benzophenone ketyl and was distilled in an atmosphere of dry nitrogen before use. NMR grade deuteriochloroform was stored over 4A molecular sieves. Lithium bis(trifluoromethylsulfonylimide) (LiN(SO<sub>2</sub>CF<sub>3</sub>)<sub>2</sub>) was a gift from 3M and was dried under vacuum at 120 °C for 24 h prior to use. All other reagents were used as received or distilled prior to use.

**Preparation of Side-Chain Ethylene Oxide Monomer.** Tri(ethylene glycol) allyl methyl ether (AMPEO<sub>3</sub>) was synthesized by the method described by Alcock et al.<sup>6</sup> and Hooper et al.<sup>18</sup> A solution of MPEO<sub>3</sub> (98.4 g, 0.6 mol) in 250 mL of THF was added dropwise to a suspension of NaH (60% dispersion in mineral oil) (28.8 g, 0.72 mol) in THF (250 mL) chilled to 0 °C. This solution was stirred for a further 2 h followed by the dropwise addition of allyl bromide (87.1 g, 0.72 mol). The resulting mixture was stirred overnight and then filtered to remove the NaBr product and excess NaH. All volatile materials were removed by rotary evaporation to yield an orange oil. This oil was dissolved in water, and unreacted MPEO<sub>3</sub> was extracted using 3  $\times$  50 mL portions of toluene. The desired

**Scheme 1. General Synthesis of the Polysiloxane Precursor Containing a Small Number of Si-H Functional Groups**


product was then extracted into chloroform from the water layer with  $3 \times 200$  mL portions of  $\text{CHCl}_3$ ; this was dried with  $\text{MgSO}_4$ , and all volatile materials were removed by rotary evaporation. 110 g (90%) of product was collected by Kugelrohr distillation (80 °C/0.5 Torr):  $^1\text{H}$  NMR ( $\text{CDCl}_3$ ),  $\delta$  (ppm): 5.85 (m, 1H), 5.15 (dd, 2H), 3.95 (d, 2H), 3.45–3.65 (m, 12H), 3.30 (s, 3H).  $^{13}\text{C}$  NMR ( $\text{CDCl}_3$ ),  $\delta$  (ppm): 134.6, 116.8, 72.1, 71.8, 70.3–70.0, 69.2, 58.9. Mass spectroscopy:  $m/e$  205  $\text{MH}^+$  base peak.

**Preparation of Allyl-PEO-Allyl Cross-Linking Agents.** The  $\alpha,\omega$ -diallyl poly(ethylene glycol) was prepared using the same reactions described above for compound AMPEO<sub>3</sub>. The following reagents and quantities were used: NaH (9.6 g, 0.24 mol of a 60 wt % solution in mineral oil), THF (100 mL), PEG ( $M_w$  600, 60.0 g, 0.10 mol), THF (150 mL), allyl bromide (31.46 g, 0.26 mol). The crude product was purified by passing through a silica gel column. Final product, 62.5 g, 92% yield.  $^1\text{H}$  NMR ( $\text{CDCl}_3$ ),  $\delta$  (ppm): 5.85 (m, 2H), 5.15 (dd, 4H), 3.95 (d, 4H), 3.45–3.65 (m, 40H), 3.30 (s, 6H).  $^{13}\text{C}$  NMR ( $\text{CDCl}_3$ ),  $\delta$  (ppm): 134.6, 116.8, 72.1, 71.8, 70.3–70.0, 69.2, 58.9.

**Preparation of Polysiloxane Precursors.** The hydrosilylation of AMPEO<sub>3</sub> with PMHS was carried out under nitrogen at 75 °C, as described elsewhere.<sup>19</sup> The ratio  $n/m$  (see Scheme 1) was varied by adjusting the molar ratio of AMPEO<sub>3</sub> and Si-H groups. In a typical reaction to synthesize the partly substituted polysiloxane precursor, 50  $\mu\text{L}$  of Pt(dvs) (100 ppm, ~2% in xylene) was syringed into the mixture of 30 g (0.5 mol of Si-H) of PMHS and 102 g (0.5 mol) of AMPEO<sub>3</sub>. The heterogeneous mixture was heated to 75 °C until no residual AMPEO<sub>3</sub> allyl protons were detected in the  $^1\text{H}$  NMR spectrum. The resulting polymer was then precipitated six times in hexane to remove side product and catalyst. Afterward, all volatiles were removed under vacuum. One peak was observed in the refractive index GPC measurement;  $M_w = 6.9 \times 10^3$  compared to polystyrene standards ( $M_w/M_n = 1.12$ ). The  $n/m$  ratio of 1/30 was determined by the ratio of the integration area of Si-H at 4.6 ppm compared to Si-CH<sub>3</sub> at 0.3 ppm from the  $^1\text{H}$  NMR spectrum. IR shows a strong absorption band at 2161  $\text{cm}^{-1}$  for  $\nu(\text{Si-H})$  and 1094  $\text{cm}^{-1}$  for  $\nu(\text{Si-O-Si})$ .  $^{29}\text{Si}$  NMR (500 MHz,  $\text{CDCl}_3$ ): -23.5 ppm of  $\text{CH}_3\text{Si-CH}_2$ , 5.9 ppm of  $(\text{CH}_3)_3\text{Si-}$ , -37.5 ppm of  $\text{CH}_3\text{SiH-O}$ .

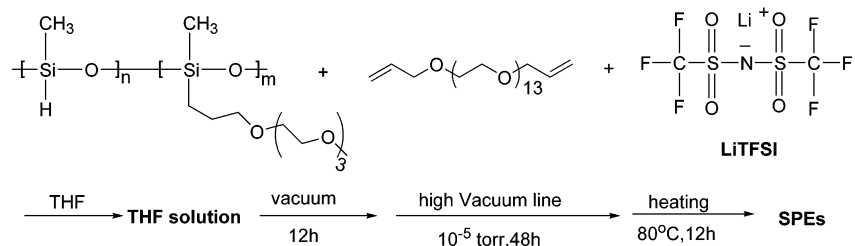
**Procedure for Preparation of Cross-Linked Polysiloxane Network Electrolytes.** In a typical preparation,<sup>20</sup> the viscous branched polysiloxane precursor with  $n/m$  ratio of 1/30 (0.514 g,  $1.74 \times 10^{-3}$  mol of Si-H) was added into dry a 10 mL flask, and then diallyl poly(ethylene glycol) cross-linker ( $q \sim 13$ ) (0.0465 g,  $8.7 \times 10^{-4}$  mol),  $\text{LiN}(\text{CF}_3\text{SO}_2)_2$  ( $2.48 \times 10^{-4}$  mol, 6.75 mL of 0.0367 M THF solution), and Pt catalyst (5  $\mu\text{L}$ ) were syringed into the flask. The mixture was stirred thoroughly. The resulting solution was evacuated for 12 h and then further evacuated on a high-vacuum line ( $\sim 10^{-5}$  Torr) for 48 h to completely remove the THF. The flask was sealed and transferred into a glovebox, where the liquid electrolyte was loaded into the conductivity measurement cell. After 12 h in an 80 °C oven, a transparent film resulted.

**Equipment.** Molecular weights and molecular weight distributions (MWDs) ( $M_w/M_n$ ) of polysiloxane precursors were determined by a Viscotek GPC instrument equipped with a series of three gel permeation columns (500, 10<sup>4</sup>, and 10<sup>5</sup> Å) calibrated with narrow MWD polystyrene standards, a Viscotek VE3580 refractive index detector, and a Viscotek T60B dual detector (viscometer detector and light scattering detector). The flow rate was 1 mL/min of HPLC grade toluene. TriSEC 2000 Data Acquisition software was used for data analysis.

All NMR chemical shifts are reported in parts per million ( $\delta$ , ppm); downfield shifts are reported as positive values from tetramethylsilane (TMS) as the standard at 0.00 ppm. The  $^1\text{H}$  and  $^{13}\text{C}$  chemical shifts are reported relative to the NMR solvent as an internal standard, and the  $^{29}\text{Si}$  chemical shifts are reported relative to an external TMS standard. NMR spectra were recorded using samples dissolved in  $\text{CDCl}_3$ , unless otherwise stated, on the following instrumentation:  $^1\text{H}$  NMR Bruker AC300 (300.1 MHz) with Grant NIH 1 S10 RRO 8389-01;  $^{13}\text{C}$  NMR Bruker AC300 (75.5 MHz) with Grant NIH 1 S10 RRO8389-01;  $^{29}\text{Si}$  NMR Varian Unity 500 (99.2 MHz) with Grants NIH 1 S10 RRO4981-01 and NIH CHE-9629688. Carbon-13 NMR was recorded as proton-decoupled spectra, and  $^{29}\text{Si}$  NMR was recorded using an inverse gate pulse sequence with a relaxation delay of 30 s.

DSC measurements were recorded on a TA Instruments model 2920 modulated DSC operated under computer control by the TA Instruments package Thermal Advantage Version 1.0A for Windows with data analyses performed on the software Universal Analysis for Windows Version 2.6D. Low temperatures were achieved by using the TA Instruments liquid nitrogen cooling accessory. Samples of preformed gels were loaded in hermetically sealed aluminum pans. Duplicates of all samples were measured. Glass transition temperatures are reported as the onset of the inflection in the heating curve from -150 to 80 °C at a heating rate of 10 °C/min. Any other thermal transitions observed for the samples were measured at their peaks.

Impedance measurements were performed under computer control using a Princeton Applied Research model 273A potentiostat/galvanostat, a Princeton Applied Research model 1025 frequency response analyzer for frequency control (75 Hz to 100 kHz), and Princeton Applied Research PowerSine impedance software for data acquisition. Subsequently, the data obtained were analyzed on a PC with Microsoft Excel. Room temperature conductivity measurements were at  $23 \pm 1$  °C while variable-temperature measurements (0–70 °C) were made by placing the electrochemical cell in a jacketed

**Scheme 2. Synthetic Procedure for a Cross-Linked Polysiloxane Electrolyte Film**

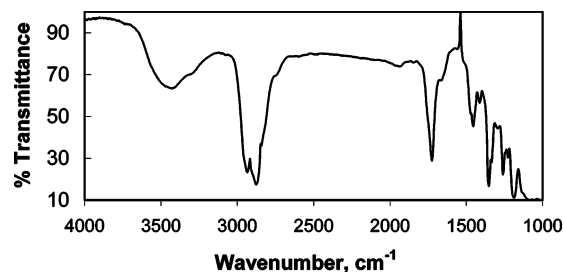



**Figure 1.** Representative FTIR of the cross-linked SPE-2 with  $\text{EO/Li}^+ = 20$ .

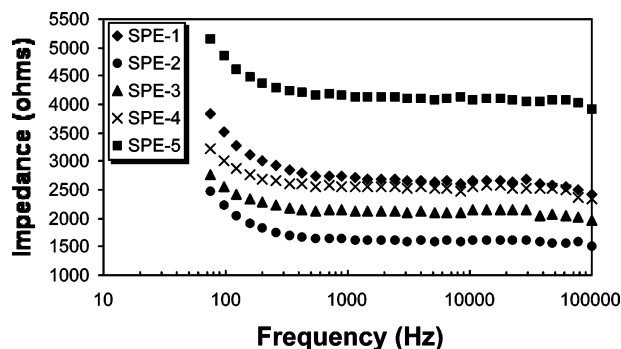


**Figure 2.** Impedance spectra of cross-linked SPEs at various LiTFSI doping levels ( $\text{EO/Li}^+ = 15:1, 20:1, 24:1, 28:1$ , and  $64:1$  for SPEs 1 to 5, respectively).

holder and circulating ethylene glycol/water from a Lauda RMT6 circulating bath. Actual temperatures were determined via an Omega thermocouple attached directly to the cell.

FTIR spectra were recorded on a Nicolet Nexus 670 spectrometer as gelled films placed on the Avatar multibounce HATR accessory.

## Results and Discussion

**Precursor Synthesis.** Cross-linkable polysiloxane precursors were synthesized (Scheme 1) by hydrosilylation catalyzed by Karstedt's catalyst and purified by precipitation in hexane until no side products were detected in both the NMR and IR spectrum. The extent of hydrosilylation and purification was monitored by  $^1\text{H}$  NMR or IR. Significant amounts (20–40% overall) of the isomeric AMPEO<sub>3</sub> (cis and trans) and the reduced alkene were found at the end of the reaction.<sup>21</sup> The proposed mechanism for the formation of olefin isomers can be attributed to the dissociation of the labile divinyltetramethyldisiloxane ligand and the subsequent generation of colloidal Pt species,<sup>22,23</sup> leading to the undesired side products and coloration of the product.

**Conductive Film Preparation.** For preparation of the network electrolytes, a THF solution of precursor, cross-linker, and LiTFSI was used to ensure better dissolution of the salt in the precursor and cross-linker. This necessitated the removal of the solvent which was achieved by vacuum-drying to a pressure  $< 5 \times 10^{-5}$  Torr. Then the viscous mixture was loaded into a two-electrode electrochemical cell with stainless steel ion blocking electrodes and sealed with O-rings. To prevent any bubble defect in the resulting thin disk of electrolyte, the viscous polymer was poured into the polypropylene containment ring instead of pipetted. After impedance measurements, the resulting cross-linked film was examined by IR and NMR spectroscopy. The film did not dissolve in  $\text{CDCl}_3$  but was swollen by the solvent. No Si–H absorbance at 4.7 ppm and  $\text{CH}_2=\text{CH}-$  resonance at 5.1 and 5.9 ppm were observed, indicating

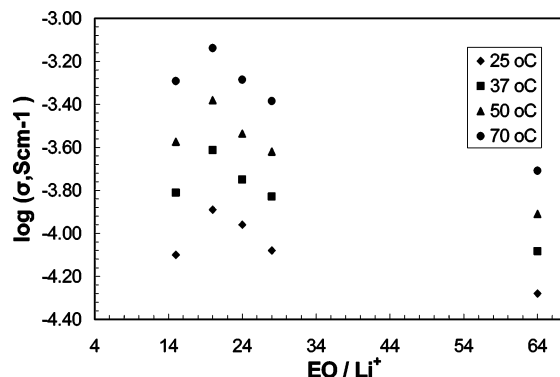


**Figure 3.** Plots of log conductivity vs  $\text{EO/Li}^+$  for SPE–LiTFSI complexes at different temperatures.

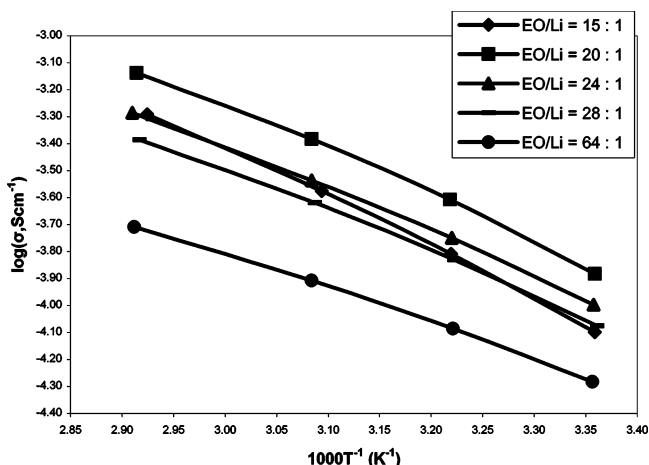


**Figure 4.** Variable-temperature conductivities for SPEs at various LiTFSI doping levels (symbols are experimental data; lines are VTF fits).

**Table 1. Conductivities for SPEs at Various LiTFSI Doping Levels**

SPE ID	<i>n/m</i>	<i>p</i>	<i>q</i>	$[\text{EO/Li}^+]$	conductivity ( $\text{S cm}^{-1}$ )	
					25 °C	37 °C
SPE-1	1/30	3	13	15/1	$8.00 \times 10^{-5}$	$1.55 \times 10^{-4}$
SPE-2	1/30	3	13	20/1	$1.33 \times 10^{-4}$	$2.44 \times 10^{-4}$
SPE-3	1/30	3	13	24/1	$1.01 \times 10^{-4}$	$1.78 \times 10^{-4}$
SPE-4	1/30	3	13	28/1	$8.38 \times 10^{-5}$	$1.48 \times 10^{-4}$
SPE-5	1/30	3	13	64/1	$5.18 \times 10^{-5}$	$8.27 \times 10^{-5}$

complete gelation of the reagents. The IR of the thin film also confirmed the completion of network formation (no Si–H stretch at  $2160 \text{ cm}^{-1}$  was observed, see Figure 1).

## Electrochemical Results

Ionic conductivities for the network electrolytes were obtained as a function of temperature from the impedance data. The impedance spectra, measured over the frequency range of 75 Hz–100 kHz, were described in an equivalent circuit of a parallel capacitance and resistance (see Figure 2).

The magnitude of the resistance was calculated at the points where the phase angle in the impedance data was closest to zero using the equation  $R = Z \cos(\theta)$ , where  $R$  is the resistance,  $Z$  the impedance, and  $\theta$  the phase angle. The conductivity,  $\sigma$ , was calculated from the relationship  $\sigma = 1/R \times l/A$ , where  $l/A$  values were typically  $0.2 \text{ cm}^{-1}$ . Transparent thin films of cross-linked polysiloxane SPE with lithium bis(trifluoromethanesulfonylimide) are ionically conductive. The LiTFSI salt-



Table 2. VTF and Thermal Parameters for SPE-1 to SPE-5

sample	EO/Li	$A$ ( $\text{S cm}^{-1} \text{K}^{1/2}$ )	$B$ ( $\text{K}^{-1}$ )	$T_0$ (K)	$E_a$ ( $\text{kJ mol}^{-1}$ )	$T_g$ (K)	$T_m$ (K)
SPE-1	15:1	0.090	865.14	197.92	7.2	213.3	259.4
SPE-2	20:1	0.032	547.44	174.70	4.5	206.5	255.0
SPE-3	24:1	0.057	834.22	176.27	4.9	204.6	265.0
SPE-4	28:1	0.023	642.76	182.98	5.3	201.2	258.7
SPE-5	64:1	0.007	590.82	166.05	6.9	193.2	256.0

complexed polymers have maximum, ambient ionic conductivities in the range from  $5.18 \times 10^{-5}$  to  $1.33 \times 10^{-4} \text{ S cm}^{-1}$  and  $8.27 \times 10^{-5}$  to  $2.44 \times 10^{-4} \text{ S cm}^{-1}$  at body temperature ( $\sim 37^\circ\text{C}$ ), as shown in Table 1. EO/Li<sup>+</sup> indicates the total number of ether oxygens (on side chains plus diallyl-terminated PEO cross-linker).

The effect of salt concentration on ionic conductivity is shown in Figure 3. For data collected in the temperature range  $25\text{--}70^\circ\text{C}$ , the conductivity increases with increasing salt concentration from ether oxygen/lithium ratio 64:1 to 20:1, apparently due to an increase in the number of charge carriers. As the LiTFSI concentration increases beyond 20:1, the conductivity decreases. The maximum conductivity ( $\sigma_{\text{RT}} = 1.33 \times 10^{-4} \text{ S cm}^{-1}$ ) was found to occur with the electrolyte that contained a LiTFSI concentration of EO/Li<sup>+</sup> = 20. Morales et al.<sup>15</sup> recently reported slightly higher room temperature conductivities of  $2.0 \times 10^{-4}$  and  $5.0 \times 10^{-4} \text{ S cm}^{-1}$  for monocomb polysiloxane–LiTFSI complexes of PMMS3M and PMMS12M, respectively; however, these values occurred at a higher salt concentration (O:Li ratio of 10:1) compared with that of the cross-linked polymer. The dependence of the ionic conductivity on doping level can be adequately interpreted by two opposing effects. There is a buildup of charge carriers as the salt concentration is increased, but this is eventually offset by a decrease in the flexibility of the polymer network which will impede the ion migration in the network polymer electrolytes.

The temperature dependence of the ionic conductivity is shown in Figure 4 for SPEs with salt concentrations of EO/Li = 64:1, 28:1, 24:1, 20:1, and 15:1. They show the obvious trend, whereby conductivities increase with increasing temperature. For the five complexes, Arrhenius plots all had the curvature characteristic of ion transport dependent on the segmental motion of the oligoether chain as well as the polysiloxane backbone. The Vogel–Tamman–Fulcher<sup>24</sup> (VTF) equation

$$\sigma = AT^{-1/2}e(-B/(T - T_0))$$

has been used to fit the behavior of the temperature-dependent conductivities of these SPE materials. Table 2 lists the values of the parameters  $A$ , reflecting the number of charge carriers,  $B$ , the apparent activation energy, and  $T_0$ , the ideal glass transition temperature. The  $T_0$  values are all closer to the experimental  $T_g$  than the typical 50 K below  $T_g$ .

Thermal properties of the SPEs are characterized by DSC measurement and are also listed in Table 2. The major thermal feature observed was a large glass transition (see Figure 5). As expected for a polysiloxane,  $T_g$  was lower than poly(ethylene oxide) and similar to other polysiloxane polymers. The glass transition temperature increased with doping level, as is typical for polymer electrolytes.

The VTF parameters and glass transition temperatures clearly correlate well with the conductivity results;  $T_g$  increases with the increasing salt concentration, with the maximum  $T_g$  (213.3 K) occurring at EO/Li<sup>+</sup> = 15:1,

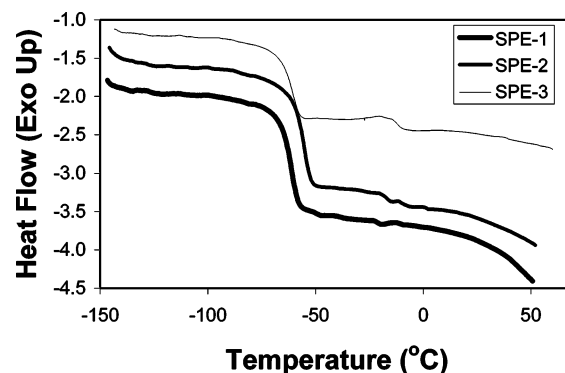


Figure 5. Thermograms for SPE-1 to SPE-3.

the highest doping level, which lowers the ionic conductivity for the complexes. In the DSC thermograms, very weak recrystallization and melt transitions ( $T_m$ ) were observed in all the cross-linked network electrolyte samples. These features were very small and at temperatures well below ambient. This confirms that the gels are amorphous over the temperature ranges where the ionic conductivity measurements were performed. Interestingly, the recrystallization and melt transitions were smaller than Morales observed in his linear polymer samples.<sup>15</sup> Formation of the cross-links in the gel may decrease the organization of the pure polymer chains and enhance the amorphous character of the polymer electrolytes. The activation energies,  $E_a$ , range from 4.5 to 7.2 kJ/mol, which are much lower compared with those reported by Shriver and co-workers<sup>12</sup> for their cross-linked siloxane (30) (from 27.9 to 46.2 kJ/mol) at various  $\text{LiSO}_3\text{CF}_3$  concentrations. This may account for their relative lower conductivities. The maximum conductivity for the SPE-2 with doping level of 20:1 occurred at  $E_a = 4.5$  kJ/mol, the lowest activation energy over the lithium salt doping range.

Our ongoing investigations indicate the cross-linking density as well as chain length of the oligo(ethylene glycol) plays an important role in enhancing the ionic conductivity of these network polymer electrolytes. Another paper will focus on these effects in the near future.

## Conclusions

Cross-linked network polymer electrolytes based on a polysiloxane backbone have been synthesized and their ionic conductivities measured when doped with LiTFSI. The solid polysiloxane network polymer electrolytes display ionic conductivities comparable to those of their liquid polysiloxane counterparts. The highest  $25^\circ\text{C}$  conductivity ( $\sigma_{\text{RT}} = 1.33 \times 10^{-4} \text{ S cm}^{-1}$ ) occurred for the electrolyte with a doping level EO/Li<sup>+</sup> of 20:1 and an activation energy of 4.5 kJ/mol, the lowest one over the lithium salt doping range. With improved mechanical properties, these solid electrolyte materials may find application as both the separator and electrolyte in lithium electronic devices.

**Acknowledgment.** This work was supported by grants from the University of Wisconsin-Industry Rela-

tions program-Advanced Technology Program (ATP) and NIST-ATP. We also thank 3M Co. for the gift of  $\text{LiN}(\text{CF}_3\text{SO}_2)_2$ . Instrumentation at Grinnell was funded by the NSF-MRI program (Grant No. 0116159). L.J.L. thanks Professor David Johnson and his students, Fred Harris and John Thompson, for use of their DSC instrument at the University of Oregon.

## References and Notes

- (1) Fenton, D. E.; Parker, J. M.; Wright, P. V. *Polymer* **1973**, *14*, 589.
- (2) Wright, P. V. *Br. Polym. J.* **1975**, *7*, 319.
- (3) Wright, P. V. *J. Polym. Sci., Polym. Phys. Ed.* **1976**, *14*, 955.
- (4) Blonsky, P. M.; Shriver, D. F.; Allcock, H. R.; Austin, P. J. *J. Am. Chem. Soc.* **1984**, *106*, 6854.
- (5) Allcock, H. R.; Napierala, M. E.; Cameron, C. G.; O'Connor, S. J. M. *Macromolecules* **1996**, *29*, 1951.
- (6) Allcock, H. R.; O'Connor, S. J. M.; Olmeijer, D. L.; Napierala, M. E.; Cameron, C. G. *Macromolecules* **1996**, *29*, 7544.
- (7) Allcock, H. R.; Ravikiran, R.; O'Connor, S. J. M. *Macromolecules* **1997**, *30*, 3184.
- (8) Allcock, H. R.; Olmeijer, D. L.; O'Connor, S. J. M. *Macromolecules* **1998**, *31*, 753.
- (9) Khan, I. M.; Yuan, Y.; Fish, D.; Wu, E.; Smid, J. *Macromolecules* **1988**, *21*, 2684.
- (10) Zhou, G. B.; Khan, I. M.; Smid, J. *Macromolecules* **1993**, *26*, 2202.
- (11) Fish, D.; Khan, I. M.; Wu, E.; Smid, J. *Br. Polym. J.* **1988**, *20*, 281.
- (12) Spindler, R.; Shriver, D. F. *Macromolecules* **1988**, *21*, 648.
- (13) Spindler, R.; Shriver, D. F. *J. Am. Chem. Soc.* **1988**, *110*, 3036.
- (14) Siska, D. P.; Shriver, D. F. *Chem. Mater.* **2002**, *13*, 4698.
- (15) Morales, E.; Acosta, J. L. *Electrochim. Acta* **1999**, *45*, 1049.
- (16) Hooper, R.; Lyons, L. J.; Moline, D. A.; West, R. *Organometallics* **1999**, *18*, 3249.
- (17) Hooper, R.; Lyons, L. J.; Moline, D. A.; West, R. *Silicon Chem.* **2002**, *1*, 121.
- (18) Hooper, R.; Lyons, L. J.; Mapes, M. K.; Schumacher, D.; Moline, D. A.; West, R. *Macromolecules* **2001**, *34*, 931.
- (19) Zhang, C. X.; Laine, R. M. *J. Am. Chem. Soc.* **2000**, *122*, 6979.
- (20) Zhang, Z. C.; West, R. *Adv. Technol. Program Q. Prog. Rep.* **2002** (April 20), 9.
- (21) Marko, I. E.; Sterin, S.; Buisine, O.; Mignani, G.; Branlard, P.; Tinant, B.; Declercq, J.-P. *Science* **2002**, *298*, 204.
- (22) Arduengo, A. J.; Gamper, S. F.; Calabrese, J. C.; Davidson, F. *J. Am. Chem. Soc.* **1994**, *116*, 4391.
- (23) Arnold, P. L.; Cloke, F. G. N.; Geldbach, T.; Hitchcock, P. B. *Organometallics* **1999**, *18*, 3228.
- (24) Fulcher, G. S. *J. Am. Ceram. Soc.* **1925**, *8*, 339.

MA0349276